JACS
JOURNAL OF THE AMERICAN CHEMICAL SOCIETY

ARTICLE

pubs.acs.org/JACS

Investigation of the Photoinduced Magnetization of Copper Octacyanomolybdates Nanoparticles by X-ray Magnetic Circular Dichroism

Sophie Brossard,[†] Florence Volatron,[§] Laurent Lisnard,[§] Marie-Anne Arrio,[*,†] Laure Catala,[§] Corine Mathonière,[∥] Talal Mallah,[*,§] Christophe Cartier dit Moulin,[‡] Andrei Rogalev,[⊥] Fabrice Wilhelm,[⊥] Alevtina Smekhova,[⊥] and Philippe Sainctavit[†]

[†]Institut de Minéralogie et de Physique des Milieux Condensés, CNRS UMR 7590, and [‡]Institut Parisien de Chimie Moléculaire, CNRS UMR 7201, Université Pierre et Marie Curie, 4 place Jussieu, Case 115, 75252 Paris cedex 05, France

[§]Institut de Chimie Moléculaire et des Matériaux d'Orsay, Université de Paris-Sud 11, CNRS, 15 rue Georges Clemenceau, 91405 Orsay Cedex, France

[∥]CNRS, Université de Bordeaux, ICMCB, 87 av. Du Dr A, Schweitzer, 33608 Pessac Cedex, France

[⊥]European Synchrotron Radiation Facility, 6 rue Jules Horowitz, BP220, 38043 Grenoble Cedex, France

Supporting Information

ABSTRACT: Through an extensive set of SQUID magnetic measurements, X-ray absorption spectroscopy, and X-ray magnetic circular dichroism, we have determined the nature of the metastable photomagnetic phase in the cyano-bridged 3D network $Cs_2Cu_7[Mo(CN)_8]_4$. The photomagnetic effect is induced by the photoconversion of Mo(IV) ions in low spin (LS) configuration ($S = 0$) into Mo(IV) ions in high spin (HS) configuration ($S = 1$). The magnetic and spectroscopic measurements fully support the LS to HS conversion, whereas the previously invoked charge transfer mechanism Mo(IV) + Cu(II) ⟹ Mo(V) + Cu(I) can be completely ruled out.

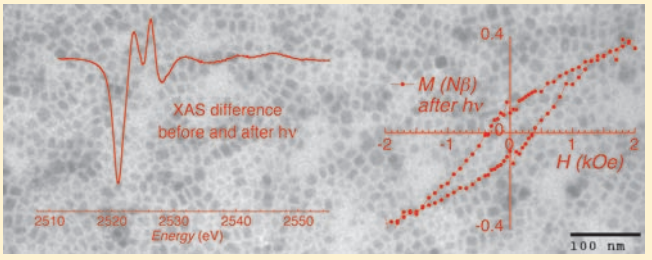

1. INTRODUCTION

Bistable magnetic coordination networks that may be tuned by various stimuli (magnetic field, light, pressure, temperature) have been the subject of intense research over the past decades.[1−6] Nanoparticles made of such networks are interesting because this bistability may be controlled at the level of a nano-object. Among the chemical compounds that can be used to form such particles, the family of cyanide-bridged coordination networks was found to be of particular interest.[7−16] Indeed, such materials are known to exhibit interesting properties such as ferromagnetism below Curie temperatures that can reach room temperature,[2,3,17] spin crossover,[4] and particularly photomagnetism:[1] upon irradiation and absorption of photons, changes in the electron configuration of the metallic ions of the structure lead to changes in the magnetic properties.[18,19]

The first compound in which photoinduced magnetization was observed was the Prussian Blue Analogue (PBA) $K_{0.2}Co_{1.4}[Fe(CN)_6]\cdot 6.9H_2O$ in which Co and Fe atoms are linked by cyanides: the fcc network consists of Fe^{II} ($S = 0$)−CN−Co^{III} ($S = 0$) pairs yielding a diamagnetic material.[5,18−24] As was first observed by Shirom et al.[25] in solution and in glasses, the $Fe(CN)_6^{4-}$ ions can be oxidised by irradiation (λ = 313 nm). For the PBA compounds, upon illumination with visible light, an electron transfer occurs from the iron ions to the cobalt ions, resulting in a metastable state formed by Fe^{III} ($S = 1/2$) and Co^{II} ($S = 3/2$) ions with a ferrimagnetic arrangement through the cyanide bridges, which relaxes to the stable state at temperature up to 120 K depending on the nature and amount of the inserted alkali.[5,18−24] Study of XANES (X-ray absorption near edge spectroscopy) spectra of the compounds at $L_{2,3}$ and K edges of Fe and Co ions showed energy shifts of the characteristics peaks and intensity modifications, providing support to the hypothesis of the electron transfer,[22,24] while the recording of XMCD (X-ray magnetic circular dichroism) signals at the Co K and Fe K edges allowed the characterization of the spin configuration and spin arrangement in the system.[26] Moreover, such an effect was found to be reversible by thermal treatment of the compound;[18,19] notably, XANES spectra before irradiation and after thermal relaxation were comparable.[22]

Another class of photomagnetic networks can be synthesized with octacyanomolybdates units as building blocks.[18,23,27] Shirom et al.[28] observed the possibility of exciting through laser irradiation $Mo^{IV}(CN)_8^{4-}$ ions in solution or in glasses, and then Hennig et al.[29,30]

Received: June 6, 2011
Published: November 17, 2011

showed that associating the $[Mo^{IV}(CN)_8]^{4-}$ ions with Cu^{II} ions led to the formation of donor/acceptor pairs with the appearance of a metal−metal charge transfer band. Following these observations, octacyanomolybdate compounds $Mo(CN)_8(CuL)_x$ ($x > 1$) were developed, in which the photomagnetic behavior was explained by the following mechanism: the ion $[Mo^{IV}(CN)_8]^{4-}$ become oxidized, upon irradiation by visible light, into $[Mo^{V}(CN)_8]^{3-}$.[18,27,30−34] While Mo^{IV} (low spin d^2) has a spin $S = 0$, Mo^{V} (d^1) has a spin of $S = 1/2$. Coupling of the molybdenum ion with Cu ions, through cyanide bridges, creates a system in which the electron transfer would transform Cu^{II} (d^9, $S = 1/2$) into Cu^{I} (d^{10}, $S = 0$), and thanks to the ferromagnetic exchange interaction between the central Mo^{V} ion and the remaining Cu^{II} ions, one would observe the magnetic behavior of a magnetically coupled system. One major implication of the charge transfer mechanism is that the magnetic moment at saturation of one formula unit should remain constant because the oxidation of one Mo^{IV} ($S = 0$) ion into a Mo^{V} ($S = 1/2$) ion is accompanied by the reduction of one Cu^{II} ($S = 1/2$) into a Cu^{I} ($S = 0$) ion. Only the shape of the magnetization curve should be modified, yielding a steeper increase at low fields due to ferromagnetic interactions.[35−37]

Recently, some of us suggested that photomagnetism in molecules derived from octacyanomolybdates would not result from a charge transfer mechanism.[38] Following the idea of tailoring magnetic properties as a function of size,[39,40] the authors investigated the photomagnetic molecule: $[Mo(CN)_6(CN{-}CuL'_2)_2]$ (L′ = *N*,*N*′-dimethyl ethylene diamine). They used XANES (X-ray absorption near edge spectroscopy) and XMCD (X-ray magnetic circular dichroism) at Mo $L_{2,3}$ edges to evaluate the orbit and spin magnetic moment of molybdenum ions.[38] XMCD measurements on photomagnetic compounds track the possible changes induced by photoconversion,[41,42] and Arrio et al. showed that after X-ray-induced photoconversion the Mo ions were high spin Mo^{IV} ($S = 1$) and not Mo^{V} ions. Consequently, it was proposed that instead of a charge transfer, the X-ray-induced photoconversion caused a spin conversion between low spin (LS) Mo^{IV} ion ($S = 0$) and high spin (HS) Mo^{IV} ion ($S = 1$). It should be noted that recent theoretical studies support this experimental finding with DFT calculations.[43]

The present study intends to apply a similar methodology to an extended network of octacyanomolybdate, $Cs_{0.5}Cu_{1.75}[Mo(CN)_8]$, which has been previously synthesized and studied by Hozumi et al. in a film prepared by electrochemistry. Hozumi et al.[44] observed after blue irradiation a magnet behavior with a coercive field ($H_c = 350$ G) larger than the one found in the parent photomagnet ($H_c = 7$ G)[34,36,45] and higher Curie temperature (23 K instead of 17 K[34,36,45]) that they related to the Cs^+ cations that would induce a double-layered structure. They attributed the photoconversion to a charge transfer mechanism. Moreover, by comparing the infrared (IR), electron spin resonance (ESR) spectra, and X-ray diffraction (XRD) patterns before laser irradiation, after irradiation, and after relaxation at room temperature, they concluded that the photomagnetic changes were fully reversible. Ma et al.[32] performed XANES on the same compound at the Cu K edge and interpreted the modification of the Cu K-edge under illumination as a Cu^{II} to Cu^{I} reduction. Their interpretation was in line with the charge transfer model upon irradiation. However, because the reversibility of the Cu K-edge signal was not investigated and no reports were made regarding the Mo $L_{2,3}$ edges, the X-ray damages cannot be ruled out on the basis of their results. In the present experiment, we have investigated nanoparticles of $[Cs_{0.5}Cu_{1.75}[Mo(CN)_8]_{1.1}]^{0.4-}$ cores surrounded by molecules of DODA where DODA stands for dimethyldioctadecyl-ammonium. Photomagnetism is induced by a 405 nm laser with no X-ray-induced photomagnetism, and great care is taken to limit the X-ray induced damages. The size of the nanoparticles (i.e., $[Cs_{0.5}Cu_{1.75}[Mo(CN)_8]_{1.1}]^{0.4-}$ cores) is 17 nm ± 3 nm and was chosen so that it is small as compared to the penetration depth of the X-rays, thus ensuring that the nanoparticles are fully probed by XAS. For the first time in these Cu−Mo photomagnetic compounds, both Mo $L_{2,3}$ edges and Cu K edge have been investigated at the same time. This gives us a more complete description of the photoinduced mechanism than the reported studies performed on similar systems and allows us to clearly identify the presence of HS Mo(IV) in the photomagnetic phase with no need for the charge transfer mechanism.

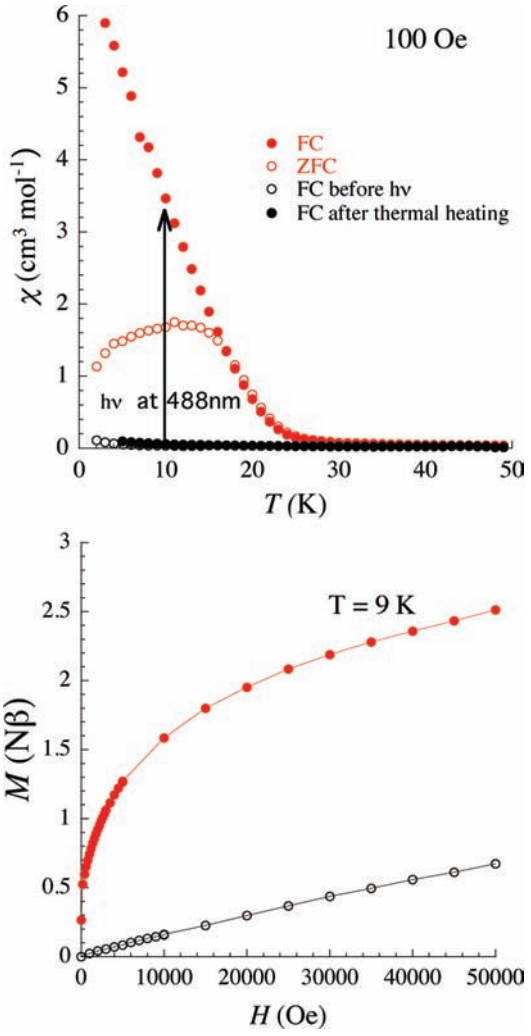

Figure 1. Magnetic measurements before (open dots) and after (full dots) illumination by a 488 nm laser per formula unit: (top) χ as a function of temperature and measured at 100 Oe; (bottom) magnetization in bohr magneton, as a function of the external magnetic field and measured at 9 K.[46,47]

2. RESULTS

2.1. Synthesis and Characterization of the Nanoparticles.

The synthetic procedure and full characterization of the particles may be found in the work published by Volatron et al.[46,47] Notably, the DODA organic cations were used to form a shell

around the $[Cs_{0.5}Cu_{1.75}[Mo(CN)_8]_{1.1}]^{0.4-}$ charged nanoparticles and facilitate their precipitation from the synthetic solution. In the following, the compound is labeled CsCuMo, and the term formula unit (f.u.) refers to a Cs:Cu:$[Mo(CN)_8]$ stoichiometry of 0.5:1.75:1.1.

The magnetic properties of the particles were first investigated using a SQUID (superconducting quantum interference device) MPMS-5S in static mode. Details on the experimental protocol are found in the work from Volatron et al.[46,47] Irradiation of the particles was carried on inside the SQUID cavity with an Ar^+-Kr^+ laser (λ = 488 nm, P = 3 mW/cm^2) coupled to an optical fiber. SQUID measurements were then made before and after a 22 h laser irradiation (see Supporting Information Figure S1a) for various temperatures and magnetic fields. The obtained curves for the magnetic susceptibility χ and the magnetization M are presented in Figure 1.

As can be seen in Figure 1, before irradiation, the magnetic susceptibility χ and the magnetization M measured at 9 K are typical of a paramagnet with the expected magnetic response of 1.75 Cu^{II} ions, the low spin Mo^{IV} ions being diamagnetic.[38,46,47] The magnetization curve displayed in Figure 1, bottom, before illumination, is consistent with the Brillouin curve calculated for 1.75 Cu^{II} ions. Irradiating the compound with a 488 nm laser significantly increases the susceptibility and the magnetization at low temperature (Figure 1top and bottom). After irradiation, the zero-field cooled and field-cooled susceptibilities present a divergence below 20 K (Figure 1, top) in agreement with the appearance of a hysteresis loop in the magnetization curve at 2 K with a coercive field around 800 Oe (see Supporting Information Figure S1b). These data confirm the magnet-like behavior of the nanoparticles. The magnetization when measured at 2 K tends to saturate at a value close to 3.1 μ_B per formula unit. When the material is heated at 200 K, the initial susceptibility and the magnetization (before irradiation) are fully recovered (Figure 1, top). These data attest the photomagnetic properties of the particles: before irradiation they show a paramagnetic behavior, while after irradiation they are clearly ferromagnetic. These photomagnetic observations are in line with the ones made on other copper octacyanomolybdate compounds.[31,34,48]

2.2. XANES and XMCD Measurements. The experiments have been performed on the ID12 beamline of the ESRF synchrotron (Grenoble, France).[49] The flux of circularly polarized photons delivered by the EMPHU undulator is monochromatized by a Si(111) two-crystal monochromator. The circular polarization rate before monochromatization (97%) drops to 12% at the Mo L_3 edge, 4% at the Mo L_2 edge, and 70% at the Cu K-edge after monochromatization.[50] The sample is magnetized by a superconducting coil delivering ±6 T and cooled to 9 K. The incoming photon flux is measured by monitoring the fluorescence of a 4 μm thick Ti foil at the Cu K edge and a thin Kapton foil at the Mo $L_{2,3}$ edges. The absorption is recorded in total fluorescence yield (TFY) by a silicon diode. More instrumental information can be found in ref 38.

The synthesized powder was here pressed in a pellet that was then glued to the copper head of the sample holder with Apiezon grease to ensure optimal thermal contact. Illumination was carried out with a laser at λ = 405 nm for 7 h (10 mW/cm^2) (ref. SHARP Blue Violet laser diode GH04020B2A mounted into a Thorlabs power supply with Thorlabs thermal regulation). The actual photon flux on the sample mounted into the variable temperature insert of ID12 cryomagnet is much less than 10 mW/cm^2 because of geometrical factors and laser divergence.

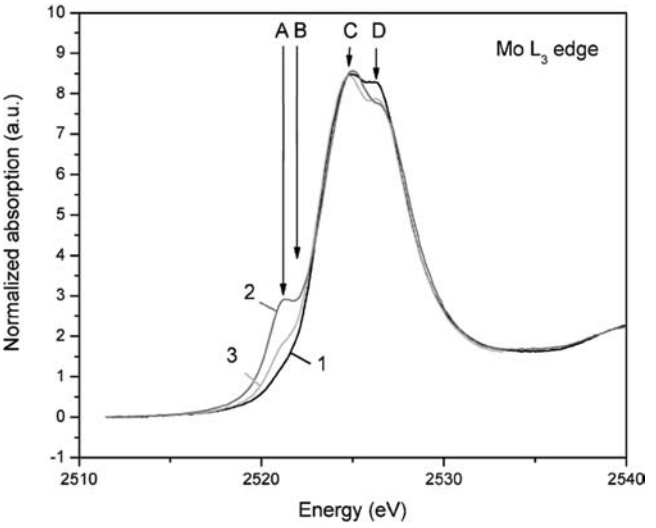

Figure 2. Absorption spectra at the Mo L_3 edge: (1) before illumination (T = 9 K); (2) after illumination (T = 9 K); and (3) after relaxation at room temperature (T = 300 K).

Previous work by Arrio et al. showed that irradiation by X-rays during such XAS experiments also induced a magnetic conversion;[38] consequently, the effects of both violet and X-ray irradiations were considered.

The XAS spectra were normalized with the following protocol: once the cross-section before the edge is set to 0 by subtraction, the edge jump in the continuum spectral region is set from 0 to 2 for the Mo L_3 edge (ΔL_3 = 2), from 2 to 3 for the Mo L_2 edge (ΔL_2 = 1), and from 0 to 1 for the Cu K edge (see the Supporting Information for more details). This allows, for the Mo $L_{2,3}$ edges, one to account for the 2/3 statistic branching ratio of the continuum states. Indeed, with the spin−orbit coupling, the 2p core level is split into two states: $j = \ell + s = 3/2$ (L_3 edge, 4-fold degeneracy) and $j = \ell - s = 1/2$ (L_2 edge, 2-fold degeneracy), leading to a $\Delta L_3/(\Delta L_2 + \Delta L_3)$ branching ratio of 2/3.

The XMCD signal has been measured by reversing both the photon helicities and the direction of the magnetic induction and was obtained by the appropriate averaging of the various cross sections. For a given energy, the XMCD signal is the difference between the XAS spectra with right and left circularly polarized X-rays. The specimen magnetization is parallel to the photons wave vector, and in the electric dipole approximation, reversing the photon helicity is equivalent to reversing the magnetic induction. Spectra are recorded in a fixed magnetic field (either +6 or −6 T), and the circular polarization is flipped at each energy point. If we note $\sigma^{\downarrow\uparrow}$ and $\sigma^{\downarrow\downarrow}$, the absorption cross sections with right polarized circular X-rays and for a magnetic field parallel and antiparallel to the photons propagation vector, and $\sigma^{\uparrow\uparrow}$ and $\sigma^{\uparrow\downarrow}$ with left polarized X-rays, then the XMCD signal can be defined as $\sigma_{XMCD} = (\sigma^{\downarrow\uparrow} + \sigma^{\uparrow\downarrow})/2 - (\sigma^{\downarrow\downarrow} + \sigma^{\uparrow\uparrow})/2$. Such sign convention means that for a 4d transition metal like Mo, a magnetic moment parallel to the applied magnetic field results in a negative value for σ_{XMCD} at the Mo L_3 edge. For sake of comparison, the XMCD spectra presented here have been renormalized for a polarization rate equal to 100%, and self-absorption corrections due to TFY mode have also been applied. Such corrected spectra allow the calculation of the orbit and spin magnetic moments of the Mo 4d shell, by

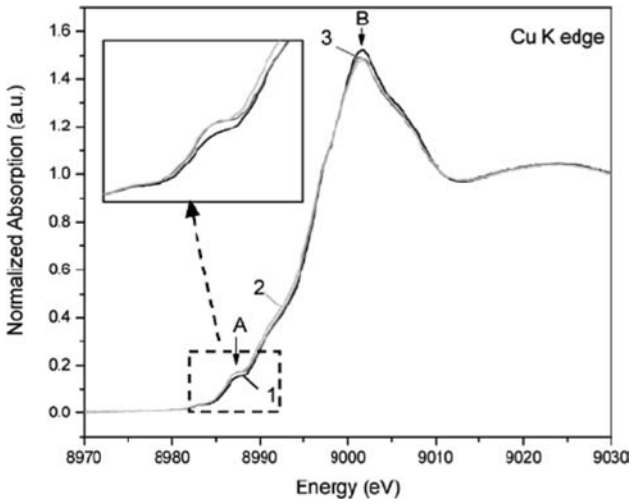

Figure 3. Absorption spectra at the Cu K edge (1) before laser illumination (T = 9 K); (2) after laser illumination (T = 9 K); and (3) after thermally induced relaxation (T = 300 K). The inset displays a zoom on the pre-edge region.

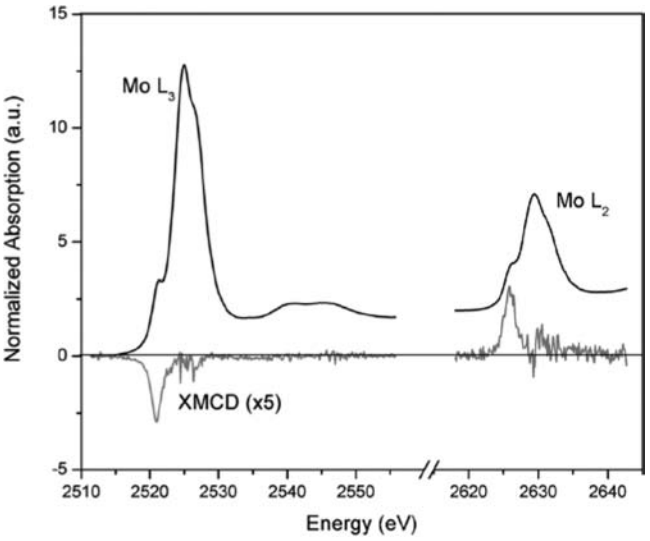

Figure 4. Isotropic XAS spectra and XMCD signals at the Mo $L_{2,3}$ edges recorded at T = 9 K and H = ±6 T. The XMCD signals have been renormalized to 100% circularly polarized X-rays and multiplied by a factor of 5.

application of the magneto-optic sum rules, as developed by Thole et al. and Carra et al.[41,42,51]

The experimental protocol is set as follow. The specimen is cooled to 9 K, and XAS spectra are measured at both Mo $L_{2,3}$ edges and Cu K edge. Laser illumination is then carried out for 7 h at 405 nm, and one then records Mo $L_{2,3}$ edges and Cu K edge at 9 K. Because the spot size of the laser is much larger than the sample, the whole sample is illuminated. Around 40 spectra are recorded at Mo $L_{2,3}$ edges for the XMCD measurements. Finally, the temperature of the specimen is raised to 300 K, and spectra at Mo $L_{2,3}$ edges and Cu K edge are measured. To study the reversibility of the photomagnetic effect, the 300 K spectra are recorded at a location on the specimen that has been laser illuminated but where no X-ray spectra have been measured.

2.3. Evolution of the Isotropic Absorption Spectra at the Mo $L_{2,3}$ Edges and Cu K Edge. Figure 2 displays the isotropic absorption spectra measured at the Mo L_3 edge before laser illumination (T = 9 K), after laser illumination (T = 9 K), and after thermally induced relaxation (T = 300 K). When comparing the spectra before and after illumination, the apparition of peak A can be noted, whereas a decrease in intensity occurs for peak D. With thermally induced relaxation (T = 300 K), one can note that the changes induced by the illumination are mostly reversible with a small nonreversible contribution. Relaxation is accompanied by a reduction of peak A with a residual contribution, and shoulder D becomes a well-defined maximum. Nevertheless, the spectrum after relaxation does not completely match the initial spectrum. Such a partial irreversibility has already been observed by Herrera et al.[27] and cannot be attributed to X-ray damages because the samples saw only a very reduced X-ray flux. Shoulder B at 2522 eV mainly corresponds to laser-induced damages because X-ray damages have also been minimized in the present experimental protocol. Similar spectra have been measured at the Mo L_2 edge (see Figure S3 in the Supporting Information), and the evolution of the various peaks is parallel to the one just described for the Mo L_3 edge. The shapes of the present XAS signals are very similar to the ones previously measured by some of us in the recent study on a related photomagnetic molecule (see Supporting Information Figure S4).[38]

Figure 3 displays the different isotropic absorption spectra measured at the Cu K edge before laser illumination (T = 9 K), after laser illumination (T = 9 K), and after thermally induced relaxation (T = 300 K). Peak A at 8987.6 and peak B at 9001.5 eV have been reported in Figure 3. With laser illumination, peak A increases and peak B decreases in intensity. The variations of intensity for peaks A and B are very small: it is around 2% of the atomic absorption for peak A and around 5% for peak B. The spectrum recorded at 300 K after thermal relaxation clearly indicates that there is no observable reversibility: the spectrum at 300 K is similar to the one measured at T = 9 K after laser illumination.

2.4. XMCD Measurements. Figure 4 reports the isotropic XAS spectra and the XMCD signal measured after laser illumination at the Mo $L_{2,3}$ egdes. Before laser illumination, the XMCD signals were nil, as expected for a diamagnetic ion. After laser illumination, a clear XMCD signal appears at the energy of feature A in Figure 2. The shape of the present XMCD signal is similar to the one previously measured on a related photomagnetic molecule.[38]

The integration of these signals and the application of the magneto-optical sum rules[51] gave the following results for the spin and orbit magnetic moments of Mo. In the hypothesis of Mo^{IV} HS (i.e., n_h, the number of 4d holes is equal to 8), one gets an orbit magnetic moment $M_L = -\mu_B\langle L_z\rangle = -0.02 \pm 0.005\ \mu_B$ and a spin magnetic moment $M_s = -g_0\mu_B\langle S_z\rangle = +0.44 \pm 0.05\ \mu_B$, which corresponds to a total magnetic moment $M = M_L + M_S = 0.42 \pm 0.06\ \mu_B$. In the hypothesis of Mo^V (n_h = 9), one gets an orbit magnetic moment $M_L = -\mu_B\langle L_z\rangle = -0.02 \pm 0.005\ \mu_B$ and a spin magnetic moment $M_s = -g_0\mu_B\langle S_z\rangle = +0.50 \pm 0.05\ \mu_B$, which corresponds to $M = M_L + M_S = 0.48 \pm 0.06\ \mu_B$.

3. DISCUSSION

Since the discovery of the photomagnetic effect in copper octacyanomolybdates, the photoinduced magnetism was attributed to a charge transfer between a low spin Mo(IV) ion and a divalent copper ion, and the scheme was said to be Mo(IV) + Cu(II) ⟹ Mo(V) + Cu(I). This mechanism was in agreement with the

dx.doi.org/10.1021/ja204594a | J. Am. Chem. Soc. 2012, 134, 222–228

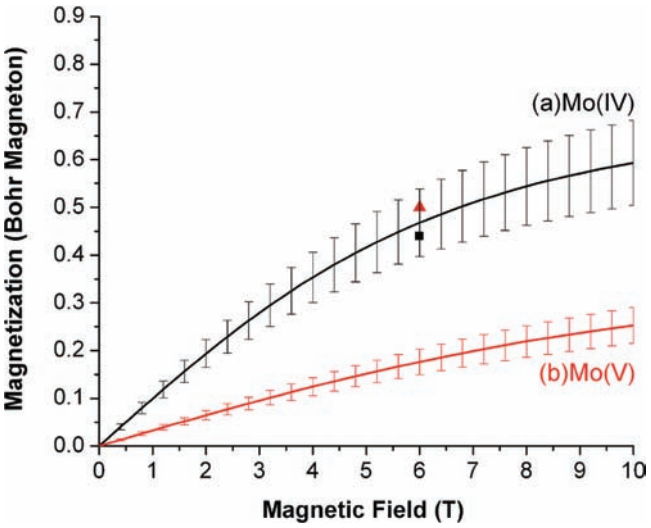

Figure 5. Theoretical spin magnetization per Mo ion for Mo(IV) ion (curve a) and for Mo(V) ion (curve b). Experimental values measured by XMCD at $H = 6$ T in the Mo(IV) hypothesis (■) and in the Mo(V) hypothesis (red ▲).

presence of a metal−metal charge transfer band in the optical spectrum. Recently, Arrio et al.[38] suggested that this picture might be not so simple. In the present discussion, we show that the charge transfer hypothesis does not hold, but that both SQUID measurements and XMCD signals can be quantitatively interpreted if the photoinduced magnetism results from a spin conversion between a low spin Mo(IV) ion and a high spin Mo(IV) ion.

Indeed, the SQUID measurements in Figure 1, bottom, clearly indicate that the magnetization per formula unit follows the expected Brillouin curve for independent $S = 1/2$ copper ions before laser illumination. Such Brillouin curve saturates at 1.75 bohr magnetons. After photoconversion, one observes a large increase of the magnetization that exceeds the magnetization at saturation before photoconversion. This is in contradiction with the Mo to Cu charge transfer for the photoconversion for which the same saturation values are expected before and after the charge transfer. On the contrary, the hypothesis of the LS ($S = 0$) to HS ($S = 1$) conversion for all Mo ions would give a magnetization at saturation around 3.95 bohr magneton per formula unit, which is compatible with the SQUID measurements (full dots of Figure 1, bottom, and Figure S1b). At this point, the charge transfer hypothesis does not hold at all, and this is also confirmed by the following analysis of the X-ray spectroscopic measurements.

From the examination of Figure 2 for Mo $L_{2,3}$ edges, one can see that peak A is the feature associated with the photoconversion. Following the intensity of peak A, one sees that reversibility is almost complete but some partial damage is observed. Because the photoexcitation is mainly induced by the 405 nm laser illumination due to a very small flux used for X-rays, the difference between spectra 1 and 3 is likely to come from damages induced by the laser. We then confirm that Mo ions are involved in the photoconversion process as previously determined by Herrera et al.[27] and Arrio et al.[38] By comparison of peak A intensity in Figure 3 with the similar features from Herrera et al. and Arrio et al.,[27,38] one can estimate that the photoconversion rate in the present study is between 30% and 40% (see Supporting Information Figure SI4). In other words, around 35% ± 5% of the molybdenum ions have been photo-transformed, and around 65% ± 5% of the Mo ions remained in the Mo(IV) low spin configuration.

From the analysis of the XMCD spectra, we have determined that the average Mo magnetic moment was $0.0525n_h$ bohr magneton ($M_{spin} \approx 0.055n_h\ \mu_B$ and $M_{orbit} \approx -0.0025n_h\ \mu_B$), where n_h is the number of 4d holes ($n_h = 8$ for Mo(IV) ion and $n_h = 9$ for Mo(V) ion). In Figure 5, we have plotted the theoretical magnetization of the Mo ion for a hypothetical high spin Mo(IV) ion in a Mo(IV)−$Cu(II)_{1.75}$ molecular entity (curve a) and for a hypothetical Mo(V) ion in a Mo(V)−Cu(I)−$Cu(II)_{0.75}$ molecular entity (curve b) considering a photoconversion yield of 35% ± 5%. The "■" in Figure 5 is the measured XMCD magnetization in the case of Mo(IV) ($n_h = 8$), and the "▲" is for the case of Mo(V) ($n_h = 9$). From Figure 4, it is clear that the hypothesis of HS Mo(IV) fits well with the experimental data: the "■" is sitting within the errors bars of curve a. On the contrary, the hypothesis of Mo(V) gives a too small calculated magnetization to explain the experimental value because the triangle is well above the curve b. The photoinduced formation of Mo(V) then is not compatible with the experimental data.

To confirm the absence of charge transfer, we measured the XAS spectra at the Cu K-edge (Figure 3). In the CsMoCu compound, there are two sites for Cu ions: Cu^{II} ions with a square-based pyramidal geometry, linked with five Mo(CN) units, and Cu^{II} ions in a square planar configuration.[44] XANES spectra allow the investigation of the valence and the local geometry of atoms. According to the literature, Cu^{I} ions are characterized by a pre-edge around 8980−8983 eV, whereas Cu^{II} ions display a pre-edge at 8986−8989 eV.[52−57] The edge peak, corresponding to peak B in Figure 3, is located 13 eV higher than the pre-edge peak A. In Figure 3, peak A (8987.1 eV) in spectrum 1 (that is before illumination) is then consistent with Cu^{II} ions. With photoillumination, one observes only small modifications of the copper pre-edge. Peak A intensity increases by 2% of the atomic absorption with no noticeable energy shift. Moreover, spectra 2 and 3 in Figure 3 are almost identical so that there is no spectroscopic evidence that Cu ions are involved in the thermally induced relaxation. The small difference between spectra 1 and 2 (2% at peak A, and 5% at peak B) is likely to come from some degradation of the sample under the laser illumination. Cu ions then are not involved in the photoinduced magnetism in the compound.

4. CONCLUSION

We have measured the photomagnetic properties of nanoparticles of the extended network $Cs_{0,5}Cu_{1,75}[Mo(CN)_8]$ by SQUID magnetometry and XMCD at Mo $L_{2,3}$ edges, and we have also recorded the XAS spectra at the Cu K edge after irradiation. The charge transfer hypothesis is not compatible with the present measurements, and the only way to interpret them is to suppose the existence of a photoinduced LS Mo(IV) to HS Mo(IV) transformation. Within this hypothesis, the large increase of the magnetization per formula unit is explained by the fact that the magnetization at saturation of the molecular unit $Cs_{0.5}Cu_{1,75}[Mo(CN)_8]$ is 1.75 μ_B before photoexcitation and 3.75 μ_B after photoexcitation. The average magnetic moment of Mo ions measured by XMCD (~0.42 μ_B) corresponds to a 35% ± 5% photoconversion of LS Mo(IV) ions into HS Mo(IV) ions. The absence of signature for the presence of Cu(I) ion at Cu K-edge and also the absence of any reversible change at the Cu K

edge clearly indicate that copper ions are not involved in the photoconversion.

It is worth noting that a light-induced HS to LS conversion at low temperature is known as the LIESST effect and has been observed mainly in Fe(II) complexes,[58] even for one possessing cyanide ligands that induce a very large crystal field.[59] Yet this is the first time where such an effect is evidenced for Mo(IV) complexes.

■ ASSOCIATED CONTENT

Supporting Information. SQUID magnetic measurements, normalization procedure, study of the X-ray-induced radiation damage, evaluation of the yield of photoconversion, and SQUID and XMCD magnetic measurements as compared to theoretical magnetization. This material is available free of charge via the Internet at http://pubs.acs.org.

■ AUTHOR INFORMATION

Corresponding Author
marie-anne.arrio@upmc.fr; talal.mallah@u-psud.fr

■ ACKNOWLEDGMENT

We acknowledge the help from Giordano Poneti and Matteo Mannini who kindly provided us with their whole 405 nm laser setup, which made the experiment possible. We thank the CNRS (Centre National de la Recherche Scientifique), the French program ANR-blanc (project MS-MCNP), and the European community (contract NMP3-CT-2005-515767 NoE "MAGMANET") for financial support.

■ REFERENCES

(1) Bonhommeau, S.; Molnar, G.; Galet, A.; Zwick, A.; Real, J. A.; McGarvey, J. J.; Bousseksou, A. *Angew. Chem., Int. Ed.* **2005**, *44*, 469.
(2) Entley, W. R.; Girolami, G. S. *Science* **1995**, *268*, 397.
(3) Ferlay, S.; Mallah, T.; Ouahès, R.; Veillet, P.; Verdaguer, M. *Nature* **1995**, *378*, 701.
(4) Niel, V.; Martinez-Agudo, J. M.; Munoz, M. C.; Gaspar, A. B.; Real, J. A. *Inorg. Chem.* **2001**, *40*, 3838.
(5) Sato, O.; Iyoda, T.; Fujishima, A.; Hashimoto, K. *Science* **1996**, *272*, 704.
(6) Verdaguer, M.; Bleuzen, A.; Marvaud, V.; Vaissermann, J.; Seuleiman, M.; Desplanches, C.; Scuiller, A.; Train, C.; Garde, R.; Gelly, G.; Lomenech, C.; Rosenman, L.; Veillet, P.; Cartier dit Moulin, C.; Villain, F. *Coord. Chem. Rev.* **1999**, *190*−*192*, 1023.
(7) Boldog, I.; Gaspar, A. B.; Martinez, V.; Pardo-Ibanez, P.; Ksenofontov, V.; Bhattacharjee, A.; Gütlich, P.; Real, J. A. *Angew. Chem., Int. Ed.* **2008**, *47*, 6433.
(8) Brinzei, D.; Catala, L.; Mathonière, C.; Wernsdorfer, W.; Gloter, A.; Stéphan, O.; Mallah, T. *J. Am. Chem. Soc.* **2007**, *129*, 3778.
(9) Catala, L.; Gacoin, T.; Boilot, J.-P.; Rivière, E.; Paulsen, C.; Lhotel, E.; Mallah, T. *Adv. Mater.* **2003**, *15*, 826.
(10) Catala, L.; Mathonière, C.; Gloter, A.; Stéphan, O.; Gacoin, T.; Boilot, J.-P.; Mallah, T. *Chem. Commun.* **2005**, *6*, 746.
(11) Catala, L.; Volatron, F.; Brinzei, D.; Mallah, T. *Inorg. Chem.* **2009**, *48*, 3360.
(12) Clavel, G.; Larionova, J.; Guari, Y.; Guérin, C. *Chem.-Eur. J.* **2006**, *12*, 3798.
(13) Frye, F. A.; Pajerowski, D. M.; Anderson, N. E.; Long, J.; Park, J. H.; Meisel, M. W.; Talham, D. R. *Polyhedron* **2007**, *26*, 2273.
(14) Larionova, J.; Salmon, L.; Guary, Y.; Tokarev, A.; Molvinger, K.; Molnar, G.; Bousseksou, A. *Angew. Chem., Int. Ed.* **2008**, *47*, 8236.
(15) Moore, J. G.; Lochner, E. J.; Ramsey, C.; Dalal, N. S.; Stiegma, A. E. *Angew. Chem., Int. Ed.* **2003**, *42*, 2741.
(16) Clavel, G.; Guari, Y.; Larionova, J.; Guerin, C. *New J. Chem.* **2005**, *29*, 275.
(17) Ferlay, S.; Mallah, T.; Ouahes, R.; Veillet, P.; Verdaguer, M. *Inorg. Chem.* **1999**, *38*, 229.
(18) Bleuzen, A.; Marvaud, V.; Mathonière, C.; Sieklucka, B.; Verdaguer, M. *Inorg. Chem.* **2009**, *48*, 3453.
(19) Sato, O. *J. Photochem. Photobiol., C: Photochem. Rev.* **2004**, *5*, 203.
(20) Escax, V.; Champion, G.; Arrio, M.-A.; Zacchigna, M.; Cartier dit Moulin, C.; Bleuzen, A. *Angew. Chem.* **2005**, *44*, 1798.
(21) Yokoyama, T.; Ohta, T.; Sato, O.; Hashimoto, K. *Phys. Rev. B* **1998**, *58*, 8257.
(22) Yokoyama, T.; Kigushi, M.; Ohta, T.; Sato, O.; Einaga, Y.; Hashimoto, K. *Phys. Rev. B* **1999**, *60*, 9340.
(23) Ohkoshi, S.-i.; Hashimoto, K. *J. Photochem. Photobiol., C: Photochem. Rev.* **2001**, *2*, 71.
(24) Cartier dit Moulin, C.; Villain, F.; Bleuzen, A.; Arrio, M.-A.; Sainctavit, P.; Lomenech, C.; Escax, V.; Baudelet, F.; Dartyge, E.; Gallet, J.-J.; Verdaguer, M. *J. Am. Chem. Soc.* **2000**, *122*, 6653.
(25) Shirom, M.; Weiss, M. *J. Chem. Phys.* **1972**, *56*, 3170.
(26) Champion, G.; Escax, V.; Cartier dit Moulin, C.; Bleuzen, A.; Villain, F.; Baudelet, F.; Dartyge, E.; Verdaguer, M. *J. Am. Chem. Soc.* **2001**, *123*, 12544.
(27) Herrera, J. M.; Bachschmidt, A.; Villain, F.; Bleuzen, A.; Marvaud, V.; Wernsdorfer, W.; Verdaguer, M. *Philos. Trans. R. Soc., A* **2008**, *366*, 127.
(28) Shirom, M.; Siderer, Y. *J. Chem. Phys.* **1973**, *58*, 1250.
(29) Hennig, H.; Rehorek, A.; Rehorek, D.; Thomas, P. *Inorg. Chim. Acta* **1984**, *86*, 41.
(30) Hennig, H.; Rehorek, A.; Rehorek, D.; Thomas, P.; Bäzold, D. *Inorg. Chim. Acta* **1983**, *77*, L11.
(31) Herrera, J. M.; Marvaud, V.; Verdaguer, M.; Marrot, J.; Kalisz, M.; Mathonière, C. *Angew. Chem.* **2004**, *116*, 5584.
(32) Ma, X.-D.; Yokoyama, T.; Hozumi, T.; Hashimoto, K.; Ohkoshi, S.-i. *Phys. Rev. B* **2005**, *72*, 094107.
(33) Rehorek, D.; Salvetter, J.; Hantschmann, A.; Hennig, H.; Stasicka, Z.; Chodkowska, A. *Inorg. Chim. Acta* **1979**, *37*, L471.
(34) Ohkoshi, S.-i.; Machida, N.; Zhong, Z. J.; Hashimoto, K. *Synth. Met.* **2001**, *122*, 523.
(35) Mathonière, C.; Kobayashi, H.; Le Bris, R.; Kaïba, A.; Bord, I. *C. R. Chimie* **2008**, *11*, 665.
(36) Rombaut, G.; Verelst, M.; Golhen, S.; Ouahab, L.; Mathonière, C.; Kahn, O. *Inorg. Chem.* **2001**, *40*, 1151.
(37) Rombaut, G.; Mathonière, C.; Guionneau, P.; Golhen, S.; Ouahab, L.; Verelst, M.; Lecante, P. *Inorg. Chim. Acta* **2001**, *326*, 27.
(38) Arrio, M.-A.; Long, J.; Cartier dit Moulin, C.; Bachschmidt, A.; Marvaud, V.; Rogalev, A.; Mathonière, C.; Wilhelm, F.; Sainctavit, P. *J. Phys. Chem. C* **2010**, *114*, 595.
(39) Christou, G.; Gatteschi, D.; Hendrickson, D. N.; Sessoli, R. *MRS Bull.* **2000**, *25*, 66.
(40) Gatteschi, D. *J. Alloys Compd.* **2001**, *317*−*318*, 8.
(41) Carra, P.; Thole, B. T.; Altarelli, M.; Wang, X. *Phys. Rev. Lett.* **1993**, *70*, 694.
(42) Thole, B. T.; Carra, P.; Sette, F.; van der Laan, G. *Phys. Rev. Lett.* **1992**, *68*, 1943.
(43) Carjaval, M.-A.; Reguero, M.; De Graaf, C. *Chem. Commun.* **2010**, *46*, 5737. Carjaval, M.-A.; Caballol, R.; de Graff, C. *Dalton Trans.* **2011**, *40*, 7295.
(44) Hozumi, T.; Hashimoto, K.; Ohkoshi, S.-i. *J. Am. Chem. Soc.* **2005**, *127*, 3864.
(45) Volatron, F.; Catala, L.; Rivière, E.; Gloter, A.; Stéphan, O.; Mallah, T. *Inorg. Chem.* **2008**, *47*, 6584.
(46) Volatron, F. Ph.D. thesis, Université Paris Sud 11, 2010.
(47) Volatron, F.; Heurtaux, D.; Catala, L.; Mathonière, C.; Gloter, A.; Stéphan, O.; Repetto, D.; Clemente-Léon, M.; Coronado, E.; Mallah, T. *Chem. Commun.* **2011**, *47*, 1985.

(48) Ohkoshi, S.-i.; Tokoro, H.; Hozumi, T.; Zhang, Y.; Hashimoto, K.; Mathonière, C.; Bord, I.; Rombaut, G.; Verelst, M.; Cartier dit Moulin, C.; Villain, F. *J. Am. Chem. Soc.* **2006**, *128*, 270.
(49) http://www.esrf.eu/UsersAndScience/Experiments/ElectStructMagn/ID12/.
(50) Lefebvre, D.; Sainctavit, P.; Malgrange, C. *Rev. Sci. Instrum.* **1994**, *65*, 2556.
(51) Thole, B. T.; van der Laan, G. *Phys. Rev. A* **1988**, *38*, 38.
(52) Kurisaki, T.; Matsuo, S.; Yamashige, H.; Wakita, H. *J. Mol. Liq.* **2005**, *119*, 153.
(53) Studer, F.; Bourgault, D.; Martin, C.; Retoux, R.; Michel, C.; Raveau, B.; Dartyge, E.; Fontaine, A. *Physica C* **1989**, *159*, 609.
(54) Soderholm, J.; Goodman, G. L. *J. Opt. Soc. Am. B* **1989**, *6*, 483.
(55) Kau, L.-S.; Spira-Solomon, D. J.; Penner-Hahn, J. E.; Hodgson, K. O.; Solomon, E. I. *J. Am. Chem. Soc.* **1987**, *109*, 6433.
(56) Benzekri, A.; Cartier, C.; Latour, J.-M.; Limosin, D.; Rey, P.; Verdaguer, M. *Inorg. Chim. Acta* **1996**, *252*, 413.
(57) Irie, H.; Kamiya, K.; Shibanuma, T.; Miura, S.; Tryk, D. A.; Yokoyama, T.; Hashimoto, K. *J. Phys. Chem. C* **2009**, *113*, 10761.
(58) Decurtins, S.; Gutlich, P.; Kohler, C. P.; Spiering, H.; Hauser, A. *Chem. Phys. Lett.* **1984**, *105*, 1.
(59) Guionneau, P.; Le Gac, F.; Kaiba, A.; Costa, J. S.; Chasseau, D.; Létard, J. F. *Chem. Commun.* **2007**, 3723. Sanchez, J. S.; Balde, C.; Carbonera, C.; Denux, D.; Wattiaux, A.; Desplanches, C.; Ader, J.-P.; Gütlich, P.; Létard, J. F. *Inorg. Chem.* **2007**, *46*, 4114.